This is a peer-reviewed, accepted author manuscript of the following research article: Esposito, A & Lappa, M 2026, A new flow process model for aerothermal facilities driven by industrial plasma torches. in 27th AIAA International Space Planes and Hypersonic Systems and Technologies Conference. AIAA American Institute of Aeronautics and Astronautics, Reston, VA. https://doi.org/10.2514/6.2026-5042
Copyright © 2026 by the American Institute of Aeronautics and Astronautics, Inc. All rights reserved.

A new flow process model for Aerothermal Facilities driven by Industrial Plasma Torches

Antonio Esposito[1,a *], Marcello Lappa[2,b]

[1]Department of Industrial Engineering, University of Naples Federico II

Via Claudio 21, 80125 Naples (Italy)

[2]Department of Mechanical and Aerospace Engineering, University of Strathclyde, G11XJ Glasgow, UK

[a]antespos@unina.it, [b]marcello.lappa@strath.ac.uk

SUMMARY

In many aerothermal facilities developed to reproduce atmospheric and planetary reentry conditions, the availability of a flow-process paradigm capable of providing a rapid and accurate characterization of the thermo-fluid-dynamic environment experienced by the test article is of fundamental importance. In particular, for high-enthalpy flows generated from reservoirs at pressures below 0.5 atm, the Frozen Sonic Flow Model (FSFM), in the formulation originally proposed by Pope, has proven especially effective. Nevertheless, a major limitation of the FSFM lies in the simplified representation of the plasma torch, namely the electric arc, which has traditionally been assumed to behave as a single-flow configuration. The present study addresses this issue by introducing a two-flow formulation, thereby enabling the representation of the intrinsic heterogeneities that characterize arc-generated flows. The Pope model is subsequently applied within the mixing chamber to estimate the total enthalpy distribution along the centerline of the resulting mixed stream. Finally, the flow properties at the exit of the supersonic nozzle are determined using isentropic flow relations. Taken together, these modeling stages establish a new comprehensive strategy for the characterization of the entire aerothermal facility, spanning the arc heater, the mixing chamber, and the supersonic nozzle, while providing a more realistic description of the overall thermodynamic and fluid-dynamic processes governing the generation of high-enthalpy flows.

Keywords: #Aerothermodynamics**,** Hypersonic Tunnel, Plasma Torch

1. INTRODUCTION

Aerothermal facilities intended to replicate atmospheric and planetary reentry environments require predictive flow models capable of rapidly and accurately describing the thermo-fluid-dynamic conditions to which the test specimen is exposed. In particular, of great interest are parameters such as the total enthalpy along the flow centerline and the pressure and heat flux at the test model's stagnation point.

It is well established that the centerline total enthalpy (H_{cl}) can be correlated with the average total enthalpy at the exit of a supersonic nozzle through various theoretical approaches.

Specifically, for high-enthalpy streams originating from low-pressure reservoirs, typically below 0.5 atm, the Frozen Sonic Flow Model (FSFM) is generally regarded as an effective approach for predicting the flow behavior during expansion. Originally developed by Winovich [1] for high-pressure, equilibrium arc-heated flows, this model was later adapted by Jorgensen [2] and Pope [3] to better describe low-pressure, frozen-flow regimes.

A more recent adaptation of this framework is due to Esposito and Lappa [4], who broadened its applicability to include polyatomic molecular systems. Building upon the foundational premises established by Vincenti and Kruger [5], this variant introduced a refined theoretical formulation based on a structured hierarchy of species-specific mole balance equations, thereby, enabling a mathematically consistent treatment of flows *involving complex molecular compositions*.

To validate this enhanced strategy, a series of dedicated tests were performed using a facility engineered to simulate the thermal and fluid dynamic environment characteristic of planetary atmospheric re-entry. The experimental campaign explored a wide enthalpy spectrum, with the mass-averaged enthalpy (H_{ne}) ranging from 5 to 30 MJ/kg. Three distinct gas mixtures were investigated. Nitrogen was employed as the high-temperature carrier gas, while cooler secondary species, namely oxygen, carbon dioxide, and methane, were individually introduced to evaluate the robustness of the model across different polyatomic configurations. The enthalpy ratios predicted by the enhanced FSFM were subsequently benchmarked against two independent diagnostic techniques: the Heating Rate Method, based on measurements of stagnation-point heat flux and impact pressure along the flow centerline interpreted through the Goulard-Pope theory; and the Calorimetric Probe Method, which enables direct determination of total enthalpy through dedicated sensing devices.

Despite these advances, a significant limitation of the FSFM, including the extension proposed by Esposito and Lappa [4], resides in the simplified physical representation of the plasma torch, namely the electric arc. Existing formulations generally rely on a single-flow description, whereby the gas emerging from the torch is treated as a homogeneous medium characterized solely by bulk properties such as total enthalpy, mass flow rate, pressure, and the corresponding derived quantities, including temperature, mean velocity, density, and chemical composition. Such an approach, however, does not explicitly account for gas ionization, which constitutes an intrinsic feature of arc-generated plasmas and may persist even under relatively low electrical power conditions. Although the resulting degree of ionization can be modest, it is seldom entirely negligible, except in the case of monatomic gases, which are of limited relevance for the simulation of atmospheric entry conditions associated with most planetary bodies in the Solar System.

This study advances the state of the art by addressing this limitation through the adoption of a two-flow model (building on the original formulation by Rat and Coudert [6]), which allows for the representation of heterogeneities inherent in arc-produced flows. Within this revised

paradigm, the plasma in the anode nozzle is treated as a quasi-steady medium composed of two thermally and electrically distinct regions: a central arc column and a surrounding, electrically insulating "cold" sheath. This outer layer separates the high-temperature plasma core from the nozzle wall. Thermal conduction across this composite system is assessed using Kirchhoff's potential, which, like electrical conductivity, is expressed as a function of the gas's specific enthalpy rather than its temperature. This thermodynamic formulation provides a more robust representation of transport properties in non-equilibrium, high-enthalpy plasmas.

Within this framework, an analytical formulation is developed to predict the radial distribution of specific enthalpy inside the anode nozzle as a function of experimentally accessible quantities, including the mass-averaged enthalpy, nozzle geometry, and the thermos-physical properties of the working gas. The model is here specialized to nitrogen plasmas, for which the two-zone representation provides an effective description of the highly non-uniform structure of the arc-heated flow. In particular, the approach captures the coexistence of distinct thermal and chemical regions that characterize the plasma generated within the arc heater.

Following the determination of the thermal, fluid-dynamic, and chemical states at the plasma torch exit through the two-flow formulation, the Pope model [3] is then applied within the mixing chamber to evaluate the total enthalpy evolution along the centerline of the mixed stream. Unlike previous implementations, the present formulation incorporates both dissociation and ionization effects into the evaluation of the effective gamma (γ) parameter, thereby extending the applicability of the model to partially ionized, high-temperature gas mixtures.

The final stage of the analysis consists of calculating the flow properties at the supersonic nozzle exit. This is accomplished using standard isentropic flow relations, which yield key parameters such as static pressure, velocity, temperature, density, and chemical composition, under the assumption of ideal, lossless expansion.

We show that, collectively, these modeling procedures establish a consistent integrated methodology for describing the complete aerothermal facility, encompassing the plasma arc heater, the mixing chamber, and the supersonic expansion nozzle. Beyond delivering standard thermodynamic and flow field information, this methodology also yields an important non-dimensional metric, namely, the ratio of the aforementioned centerline enthalpy to the mean nozzle enthalpy H_{cl}/H_n, which serves as a critical parameter for evaluating facility performance and flow uniformity in high-enthalpy experimental setups.

2. THEORETICAL FLOW MODELS

2.1 Pope's one-flow model

2.1.1 Assumptions

As a preliminary step toward the implementation of the more advanced framework outlined in the Introduction, it is useful to recall the fundamental assumptions and governing features of the model originally proposed by Pope [3].

The formulation is based on the hypothesis that, for total pressures below approximately 0.5 atm, the chemical composition of the gas undergoes a “freezing” process at the entrance of the mixing chamber and subsequently remains unchanged throughout the downstream expansion process, as schematically illustrated in Fig. 1. Within this framework, the thermochemical analysis accounts exclusively for molecular dissociation phenomena, while ionization effects are neglected. This assumption is generally justified by the relatively low degree of ionization expected under the operating conditions for which the model was originally conceived. Furthermore, the flow evolution inside the nozzle is assumed to be quasi-isentropic, thereby allowing the local thermodynamic and fluid-dynamic properties to be determined through the classical isentropic relations for compressible flow.

It is worth highlighting that, despite its simplifying assumptions, the Pope model has proven remarkably effective for the rapid characterization of high-enthalpy, low-pressure flows in aerothermal testing facilities, owing to its ability to capture the dominant thermodynamic features of the expansion process with limited computational complexity. Additional details regarding the derivation and original formulation of the model may be found in Pope’s seminal work [3].

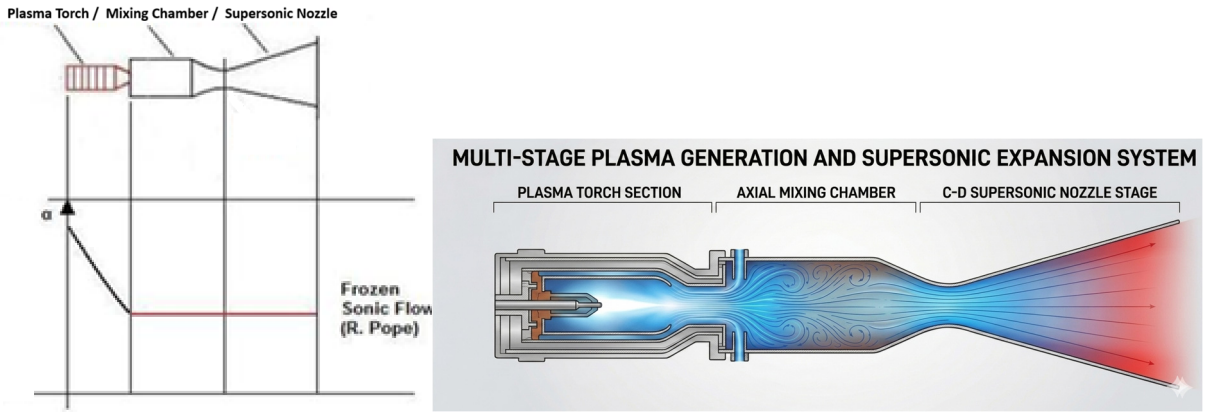

Figure 1: Pope’s one flow model

2.1.2 The Small Planetary Entry Simulator

Hardware

The experimental campaign and the associated diagnostic measurements were carried out using the SPES (Small Planetary Entry Simulator, See Fig. 2a) facility, a continuous open-circuit arc-jet system specifically developed for the simulation of atmospheric entry environments. A schematic representation of the principal components of the facility is provided in Fig. 2b.
The facility includes a gas delivery system capable of supplying total mass flow rates typically ranging between 0.5 and 1 g/s. The flow is processed through an electric arc heater based on an industrial Sulzer-Metco 9MB plasma torch equipped with arc-swirl stabilization. The torch generally operates with nitrogen as the primary working gas, although argon, helium, and their mixtures may also be employed. The maximum electrical power delivered by the system is approximately 60 kW.

a)

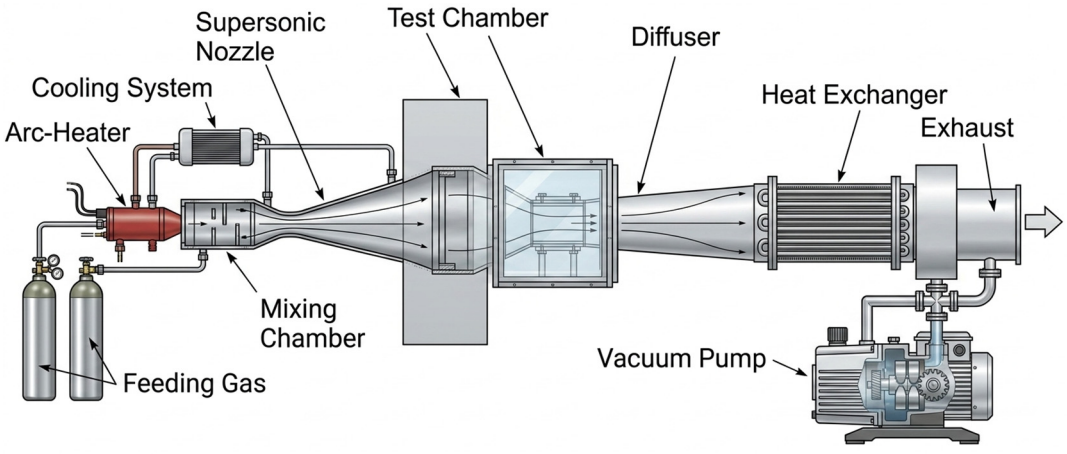

b)

Figure 2: Small Planetary Entry Simulator (SPES): (a) overall picture, (b) layout

Downstream of the plasma generator, the flow enters a mixing chamber where colder secondary gases, including oxygen and carbon dioxide, can be injected in a controlled manner to produce representative high-temperature gas mixtures relevant to planetary-entry simulations. The resulting mixture subsequently expands through interchangeable conical nozzles characterized by area ratios of 4, 20, and 56, thereby enabling operation in both supersonic and hypersonic flow regimes.

The expanded jet develops inside a cylindrical test chamber connected to a three-stage diffuser system designed to stabilize the downstream pressure field and promote efficient flow deceleration. Thermal loads are managed through a dedicated heat-exchange unit, while the required low-pressure operating conditions are maintained by a vacuum system capable of reducing the chamber pressure to approximately 10 Pa. After purification, the exhaust gases are finally released into the atmosphere.

Instrumentation

Gas mass flow rates were determined in this study using thermal mass flow meters, whereas the cooling water flow rates in both the nozzle and the arc torch were measured via variable-area flow meters. The electrical parameters of the arc heater were acquired using digital instrumentation, integrated into a dedicated data acquisition system capable of continuously recording temperatures from thermocouples distributed along the facility components. Pressure measurements were obtained through absolute pressure transducers, calibrated against a capacitive vacuum gauge to ensure traceability across the operating range.

Averaged Total Enthalpy Measurement

The bulk specific enthalpy (H) was evaluated at three axial locations within the SPES facility (see Fig. 2) using the classical energy balance method [3]. At each location, the reported enthalpy corresponds to an average value obtained from the balance of the relevant energy contributions, as summarized below:

i) The enthalpy of the gas leaving the arc-heater and entering the mixer:

$$H_{ah} = \frac{VI - (m_{H2O} C \Delta T)_{ah}}{m_{g,ah}} \quad (1)$$

This value is obtained by subtracting the thermal losses to the cooling water from the electrical input power VI, and normalizing by the mass flow rate, with the specific heat of water taken as C=4186 [J/kg].

ii) The enthalpy of the gas leaving the mixer and entering the nozzle reads:

$$H_{mc} = \frac{H_{ah} m_{g,ah} - (m_{H2O} C \Delta T)_{mc}}{m_{g,t}} \quad (2)$$

iii) The enthalpy of the flow at the nozzle exit:

$$H_{ne} = H_{mc} - \frac{(m_{H2O} C \Delta T)_{ne}}{m_{g,t}} \quad (3)$$

During each experimental run, pressures were monitored using electronic vacuum transducers at the following locations:

- p_a at the mixing chamber inlet
- p_{ne} at the nozzle exit
- p_{ts} at the test section
- p_{02} impact pressure at the stream centerline.

The overall uncertainty in the measured total enthalpy ranged from ±10% to ±20%, depending on the arc power level, while pressure measurements exhibited uncertainties between ±2% and ±5%.

2.1.3 Method Implementation

As outlined in the Introduction, the primary methodology adopted for the determination of total enthalpy is the Frozen Sonic Flow Model (FSFM). Following the formulation of Jørgensen [2], the governing relation for frozen expansion, which enables the evaluation of the total temperature T_t at the onset of the expansion, can be expressed as:

$$m_g/p_t A^* = \mathrm{CF}(\gamma)/(Z T_t)^{1/2} \quad (4)$$

where m_g and p_t are measured during the test, A^* is the sonic section and Z is the so-called compressibility factor; moreover,

$$C = m_0 / R_0 \quad (5)$$

$$F(\gamma) = [\gamma(2/\gamma+1)^{(\gamma+1)/(\gamma-1)}]^{1/2} \quad (6)$$

where γ is the isentropic exponent.

In principle, γ must be evaluated for a chemically frozen mixture comprising atomic, diatomic, and polyatomic species, including the effects of frozen vibrational modes, using the chemical composition determined from the thermodynamic state (enthalpy and pressure) at the arc-heater exit. In practice, however, this step is non-trivial and requires a more detailed thermochemical treatment, as discussed below.

To implement the FSFM in a consistent manner, the thermochemical state of the working gas must be evaluated at three key locations along the arc-jet facility: (a) the arc-heater exit, (b) the mixing chamber immediately downstream of the cold-gas injection point, and (c) the nozzle exit. The procedure is therefore organized as follows:

1. From the energy-balance measurements, the bulk enthalpies H_{ah}, H_{mc}, H_{ne} are first determined using Eqs. (1)-(3), respectively.
2. **Plasma torch:** The flow at the arc-heater exit is assumed to be in thermochemical equilibrium (Brown [7]). By taking p_a as a suitable approximation of the torch pressure and using the known value of H_{ah}, the corresponding temperature and equilibrium chemical composition can be determined with relative simplicity.
3. **Mixing chamber:** The composition downstream of the cold-gas injection point (i.e., at the effective freezing location) is evaluated using the NASA CEA code (Sanford and McBride [8]), considering the nitrogen plasma from the torch and any injected secondary gas as inputs. This step assumes instantaneous chemical equilibration under adiabatic conditions. Once the mixture composition is obtained, the compressibility factor Z and specific heat ratio γ are computed, allowing the evaluation of the total temperature T_t via Eq. (4).

Once T_t has been determined, the centerline enthalpy can finally be reconstructed using the gas composition derived from JANAF thermochemical tables [9], completing the thermodynamic characterization of the flow, with the centerline enthalpy being finally calculated as:

$$H_{CL}=\Sigma c_i\,(H_T+\Delta H_{f,T})_i \tag{7}$$

To simplify the data reduction, in general, the values of $(H_T+\Delta H_{f,T})_i$ are correlated in terms of temperature, i.e.:

$$(H_T+\Delta H_{f,T})_i=B_1T+B_2 \tag{8}$$

4. **Supersonic Nozzle**: isentropic flow formulas are used to calculate flow properties.

2.2 Rat-Pope Two-flows Model

The present variant of Pope's original Frozen Sonic Flow (FSF) methodology incorporates the two-flow formulation proposed by Rat and Coudert [6] in order to determine the flow properties at the plasma torch exit with greater physical fidelity. Within this framework, a dedicated coupling procedure is introduced to reconcile and merge the two distinct streams issuing from the arc heater into a single, effective flow state at the outlet of the mixing chamber. This intermediate reconstruction provides the necessary boundary conditions for the downstream analysis. Once this homogenized state is established, the classical Pope methodology can be consistently applied, thereby extending its applicability while preserving its original conceptual structure.

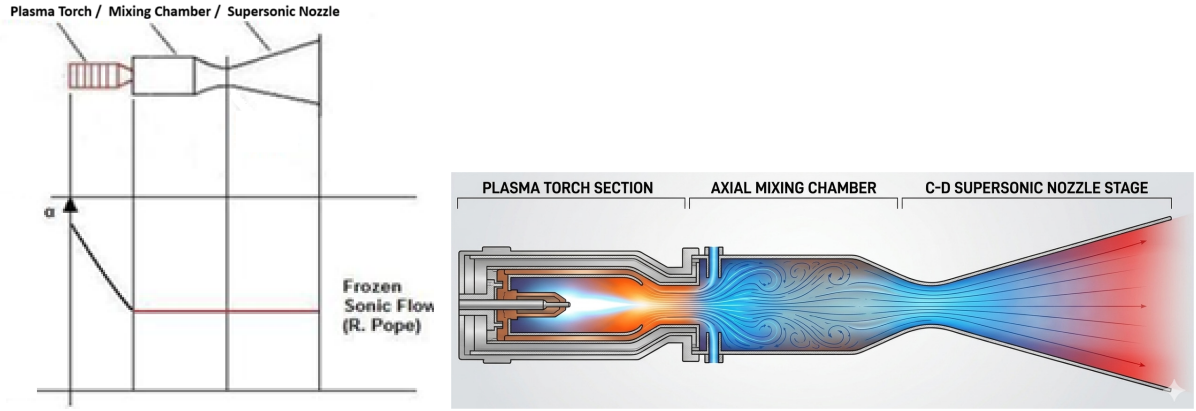

Figure 3: Rat-Pope two flows model

2.2.1 Plasma Torch

The flow in the plasma torch is divided into two concentric flows "core" and "cold layer", see Fig. 4:

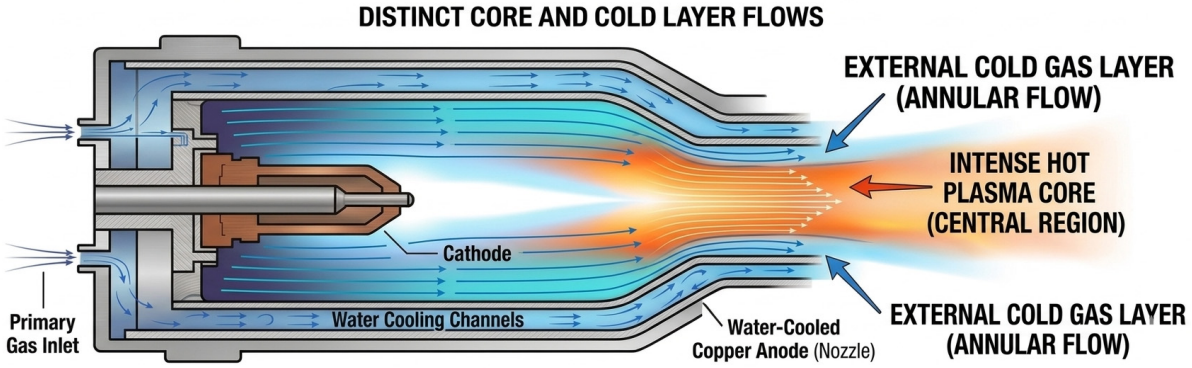

Figure 4 Rat-Coudert flow model of plasma torch

The enthalpy profile and its average for these two flows are calculated using the Rat and Coudert [6] method:

$$h = h_c + \Delta h(1-\varepsilon) \quad 0 \leq \varepsilon \leq 1 \tag{9}$$

$$h = h_c + \Delta h \ln(\varepsilon) \quad 1 \leq \varepsilon \tag{10}$$

where:

$h_c = 41.10 \frac{MJ}{kg}$

$\varepsilon = \frac{r}{r_e^2}$ with "r" radial coordinate

$\Delta h = -\frac{h_c}{(\ln y)}$ where $y = \left(\frac{r_e}{R}\right)^2$ and $R = \frac{d}{2}$ with *"d"* anode nozzle diameter.

Moreover, according to Rat and Coudert [6], the following expression can be used for the velocity profile:

$$u(r) = v^* \left(\sqrt{1 + 2\frac{h(r)}{v^{*2}}} - 1\right)$$

with $v^* = \frac{\gamma}{\gamma-1}\frac{P_a S}{m}$ and following Burm [10], γ can be conveniently chosen to be equal to 1.15.

The averaged plasma velocity at the nozzle exit reads:

$$\bar{u} = \frac{(P_{el}-P_{th})(\gamma-1)}{p_a S \gamma} \tag{11}$$

where:

P_{el} is the electrical power to the torch and P_{th} is the torch power losses

$p_a$is the pressure at mixing chamber exit and S is the cross section of the torch nozzle

Among the different factors that contribute to the torch plasma pressure, the most important one is the isentropic overpressure Δp_{is} [6]:

$$\Delta p_{is} = \frac{\bar{h}\acute{m}^2(\gamma-1)}{2\gamma S^2 p_a} \tag{12}$$

with $\acute{m}^2$ mass gas flow across the plasma torch.
Given Δp_{is},the reservoir (torch) plasma pressure can be expressed as:

$$p_0 = p_a + \Delta p_{is} \tag{13}$$

Using the enthalpy distributions, together with their corresponding averaged values, and the torch stagnation pressure p_0, all thermochemical and thermodynamic properties of the two streams are evaluated through the NASA CEA equilibrium solver. This modus operandi allows to characterize the gas in each region in terms of its equilibrium composition, temperature, and transport-related quantities.

In particular, once the density field in the core region, ρ_1, has been determined, for consistency, the density in the surrounding cold layer, ρ_2, is obtained by enforcing conservation of total mass flow rate, m, which remains constant across the two-flow configuration. Accordingly, the cold-layer density can be expressed as:

$$\rho_{2=}\frac{m-m_1}{u_1\ A_1} \tag{14}$$

Using eq. (14), the axial velocities u_1 and u_2 in the core and cold layer, respectively, are calculated. Once the velocities are known, the respective mass flow rates in the core and cold layer can be determined.

2.2.2 Mixing Chamber

By applying an overall control-volume balance between the torch inlet section (for which the previously defined thermodynamic and flow quantities are prescribed) and the outlet of the stagnation chamber (section "3"), where complete mixing between the two layers is assumed to have been achieved, a consistent set of governing relationships can be derived. Under these assumptions, the stagnation chamber is treated as a quasi-equilibrium mixing region in which mass, momentum, and energy are conserved across the two-stream system.

This formulation leads directly to the following expressions, which link the inlet conditions of the core and cold layers to the mixed flow properties at the chamber exit:

$$\alpha_3 = \frac{\sum_{i=1}^{2} m_i \alpha_i}{\sum_{i=1}^{2} m_i} \tag{15}$$

Here, the index i denotes the two flow components, namely the core and cold-layer streams, while α represents the species mass fractions, such as α_N, α_{N2} and the remaining chemical constituents provided by the CEA equilibrium calculations. The thermochemical state is

assumed to be in equilibrium within the arc region, whereas a frozen composition is imposed in the downstream direction, consistent with the adopted modeling assumptions.

$$\alpha_{N3}=\frac{\sum_{i=1}^{2} m_i \alpha_{Ni}}{\sum_{i=1}^{2} m_i},\quad \alpha_{N_2 3}=\frac{\sum_{i=1}^{2} m_i \alpha_{N_2 i}}{\sum_{i=1}^{2} m_i},\quad \alpha_{N^+ 3}=\frac{\sum_{i=1}^{2} m_i \alpha_{N^+ i}}{\sum_{i=1}^{2} m_i},\quad \alpha_{N_2^+ 3}=\frac{\sum_{i=1}^{2} m_i \alpha_{N_2^+ i}}{\sum_{i=1}^{2} m_i} \tag{16}$$

$$T_3=\frac{\sum_{i=1}^{2} m_i Cp_i T_i-\left[\left(m_{H2O} C\Delta T\right)_{ah}+\left(m_{H2O} C\Delta T\right)_{mc}\right]}{\sum_{i=1}^{2} m_i Cp_i} \tag{17}$$

In these equations, Cp_i represents the Cp provided by CEA for the core/cold layer in (initial) equilibrium conditions:

$$\rho_3=\frac{p_3}{R_3 T_3} \tag{18}$$

and R_3 is the constant determined accordingly as:

$$R_3=\frac{\sum_{i=1}^{2} m_i R_i}{\sum_{i=1}^{2} m_i} \tag{19}$$

with R_i determined for core/cold layer as: $R_i=Cp_i-Cv_i=Cp_i-\frac{Cp_i}{\gamma_i}=Cp_i\left(\frac{\gamma_i-1}{\gamma_i}\right)$, and Cp_i and γ_i provided by CEA.

The pressure at the onset of the expansion process, corresponding to the exit of the mixing chamber and here denoted as p_3 is not directly measured but is instead inferred through an extrapolation procedure. This procedure relies on two experimentally determined reference values, namely the arc-chamber pressure p_1 and the spatially averaged stagnation-chamber pressure p_{mc}, as illustrated in Fig. 5. With this approach, p_3 is obtained by reconstructing the pressure evolution along the flow path between these two sections, assuming a smooth and physically consistent variation of the thermodynamic state across the mixing region. This strategy provides a coherent estimate of the effective pressure at the beginning of the expansion, which serves as a key boundary condition for the subsequent nozzle flow analysis.

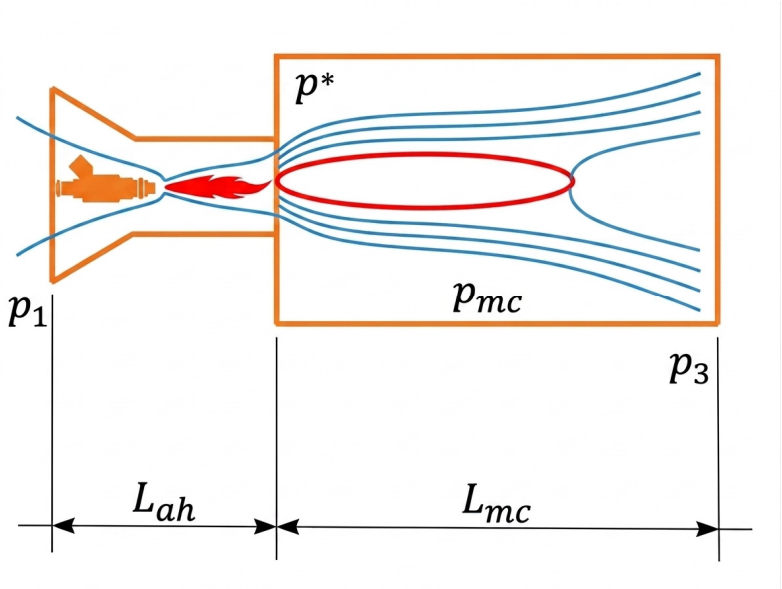

Figure 5: pressures nomenclature and location

By denoting with L_{ah} and L_{mc}, the relative lengths, the following two relations must hold (assuming that p varies linearly):

$$\frac{p_3 + p^*}{2} = p_{mc} \quad ; \quad \frac{p_3 - p^*}{L_{mc}} = \frac{p^* - p_1}{L_{ah}} \tag{20}$$

Hence:

$$p_3 = \frac{\left[2P_{mc}\left(1+\frac{L_{mc}}{L_{ah}}\right) - P_0\frac{L_{mc}}{L_{ah}}\right]}{\left(2+\frac{L_{mc}}{L_{ah}}\right)} \tag{21}$$

So, to recap:

$$\alpha_3 = \frac{\sum_{i=1}^{2} m_i \alpha_i}{\sum_{i=1}^{2} m_i} \tag{22}$$

$$T_3 = \frac{\sum_{i=1}^{2} m_i Cp_i T_i - \left[\left(m_{H2O} C\Delta T\right)_{ah} + \left(m_{H2O} C\Delta T\right)_{mc}\right]}{\sum_{i=1}^{2} m_i Cp_i} \tag{23}$$

$$p_3 = \frac{\left[2p_{mc}\left(1+\frac{L_{mc}}{L_{ah}}\right) - p_1 \frac{L_{mc}}{L_{ah}} \right]}{\left(2+\frac{L_{mc}}{L_{ah}}\right)} \tag{24}$$

$$\rho_3 = \frac{p_3}{RT_3} \tag{25}$$

2.2.3 Supersonic Nozzle

The isentropic flow formulas are used as in the previous cases (Pope's one-flow model).

3. PROCESS CODE IMPLEMENTATION

3.1 Pope's model (*Pope*)

The initial version of the computational code has been organized into a modular sequence of processing stages, each corresponding to a specific region of the arc-jet facility and the associated thermo-fluid-dynamic model, as further illustrated in the following.

a) INPUT section
This module compiles all experimental input data and performs the preliminary thermodynamic reconstruction of the flow. In particular, the average total enthalpies H_{ah}, H_{mc}, H_{ne} are evaluated using the energy balance method applied to the arc-heater, mixing chamber, and nozzle exit, respectively.

b) DEVICE OUTPUT section
This section processes the results of the energy balance together with the measured pressure data. It also provides a first-order estimate of the pressure at the onset of expansion (p_t, appearing in eq. (4)), based on an empirical correlation derived for arc-heated flows. This estimate serves as an initial boundary condition for the downstream flow reconstruction.

c) TORCH section
In this module, the thermodynamic state at the plasma torch exit is determined. The total enthalpy H_{ah} is obtained directly from the energy balance, while the corresponding stagnation pressure p_0 is evaluated using Eq. (13). The kinetic energy contribution is explicitly separated from H_{ah} in order to recover the static enthalpy h_{ah}.

Using the resulting pair of state variables (h_{ah}, p_0), the T–p formulation of the NASA CEA code is employed to compute the equilibrium chemical composition and associated thermophysical properties, including density, isentropic exponent γ, specific heats (both equilibrium and frozen), and the local speed of sound. The mean flow velocity is then obtained from $m/\rho S$, where m is the mass flow rate, ρ is the gas density, and S is the cross-sectional area of the torch nozzle.

d) MIXING CHAMBER section

This module evaluates the flow state at the chamber exit under the assumption of frozen chemistry across the mixing region. Accordingly, the chemical composition is taken to be identical to that computed at the torch exit, while the thermodynamic properties are updated consistently with the mixing process and the imposed conservation constraints.

e) SUPERSONIC NOZZLE section

The final module determines the flow properties at the nozzle exit, where the expansion is treated using appropriate compressible flow relations consistent with the adopted modeling assumptions.

This modular architecture is preserved in the extended Rat-Pope formulation, albeit with targeted modifications to account for the improved representation of the two-flow structure and mixing dynamics.

3.2 Two-flows Model (*Rat-Pope*)

The second version of the computational code introduces a revised formulation with respect to the original implementation, primarily affecting the treatment of the upstream plasma generation and subsequent mixing processes.

c) TORCH section

In this updated version, the thermodynamic and flow conditions at the torch exit are no longer evaluated under a single-stream assumption. Instead, they are determined using the two-flow model [6], which resolves the plasma jet into a core region and the surrounding cold layer. This approach enables a more detailed representation of the intrinsic non-uniformities of the arc-heated flow, providing separate but coupled descriptions of the two streams emerging from the plasma torch.

d) MIXING CHAMBER section

Within the mixing chamber, the flow evolution is treated through an explicit merging procedure of the core and cold-layer properties. The two streams are combined into a single effective state

at the chamber exit by enforcing conservation principles and consistency of the relevant thermodynamic variables. This reconstructed mixed state provides the boundary conditions required for the downstream expansion analysis and represents the first stage at which the flow can be treated as effectively homogenized.

4. RESULTS - PRESENTATION AND DISCUSSION

4.1 Comparison between Pope and Rat-Coudert models

4.1.1 Plasma Torch

A direct comparison between the two modeling approaches is not straightforward, since the underlying representations of the plasma torch differ fundamentally as extensively explained in the preceding sections, the Pope formulation is based on a single-stream description, whereas the Rat-Coudert model [6] adopts a two-flow framework, explicitly resolving a high-energy core region and a surrounding cold layer.

Figures 6(a) and 6(b) illustrate the total enthalpy and velocity distributions predicted by the Rat-Coudert model [6] at the plasma torch exit for two distinct operating conditions. The results highlight the strongly non-uniform structure of the emerging jet, with pronounced gradients between the energetic core and the comparatively cooler peripheral region. In particular, it is observed that increasing the electrical power input leads to a marked enlargement of the core region relative to the cold layer. This behavior is accompanied by a corresponding redistribution of both enthalpy and momentum, indicating a progressive dominance of the high-energy central flow as the torch operating conditions become more intense.

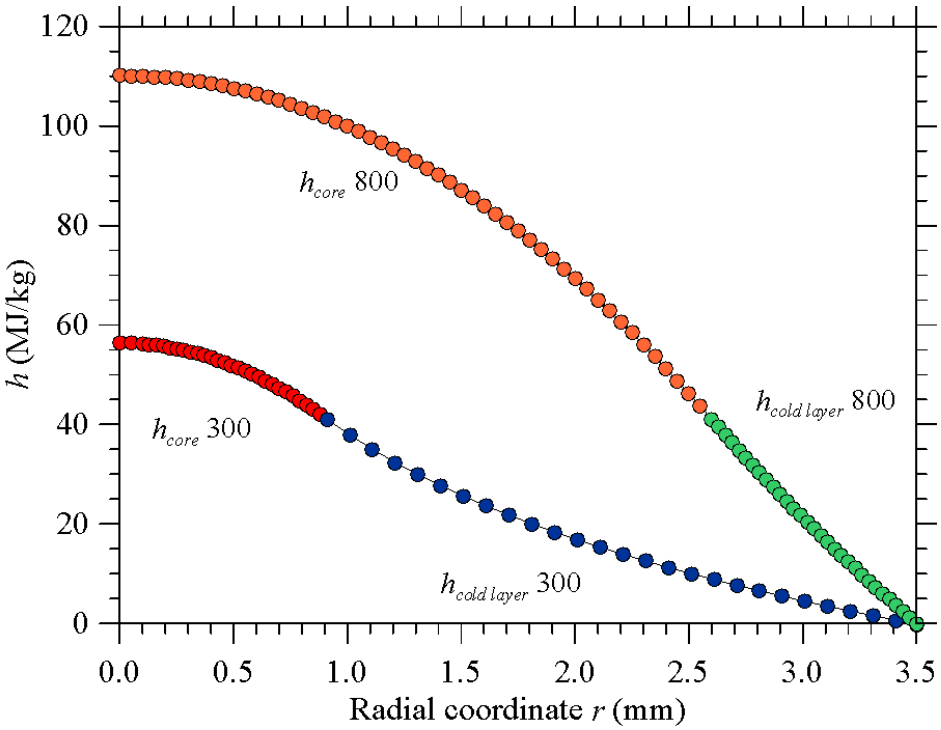

(a) Profiles of local enthalpies

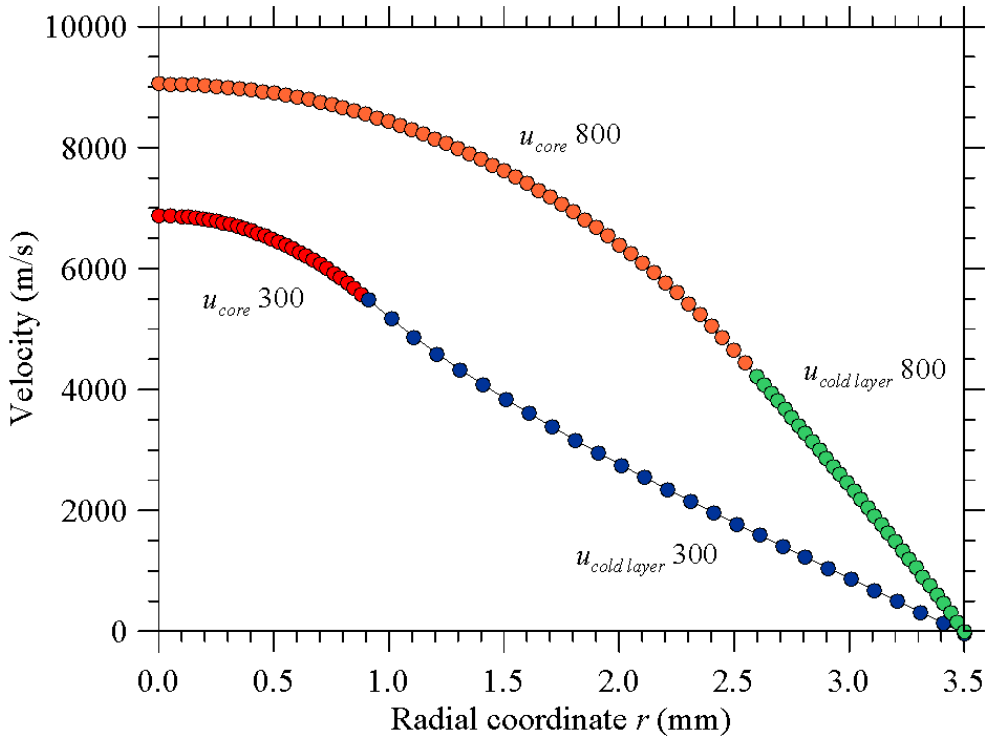

(b) Profiles of axial velocities

Figure 6: Profiles of enthalpy and velocity for the Rat model at two different arc power levels

4.1.2 *Mixing Chamber*

Figures 7, 8, and 9 present the outcomes of the calculations for nitrogen at a mass flow rate of 0.5 g/s, with total enthalpy values H_n spanning 10 to 40 MJ/kg. The comparisons include the standard Pope model, which relies on a single flow without ionization (blue line), and the newly developed Rat-Pope formulation, the above-mentioned two-flow model incorporating ionization, often termed the "core-cold layer" approach (red line). The intermediate case is also shown, consisting of the improved one-flow Pope model in which the chemical composition is evaluated using the well-established CEA code [11], with ionization effects included (green line). The results demonstrate that the classical Pope method significantly underestimates the centerline enthalpy, while the modified one-flow and two-flow formulations yield clearly distinguishable predictions.

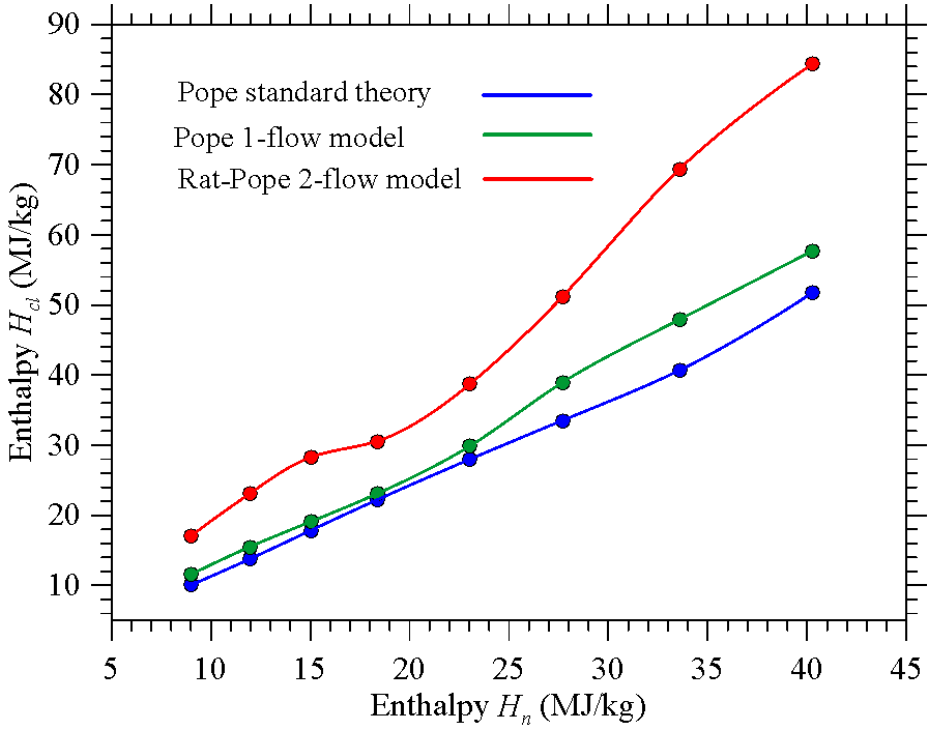

Figure 7: Enthalpy H_{cl} as a function of H_n (the splines are used to guide the eye).

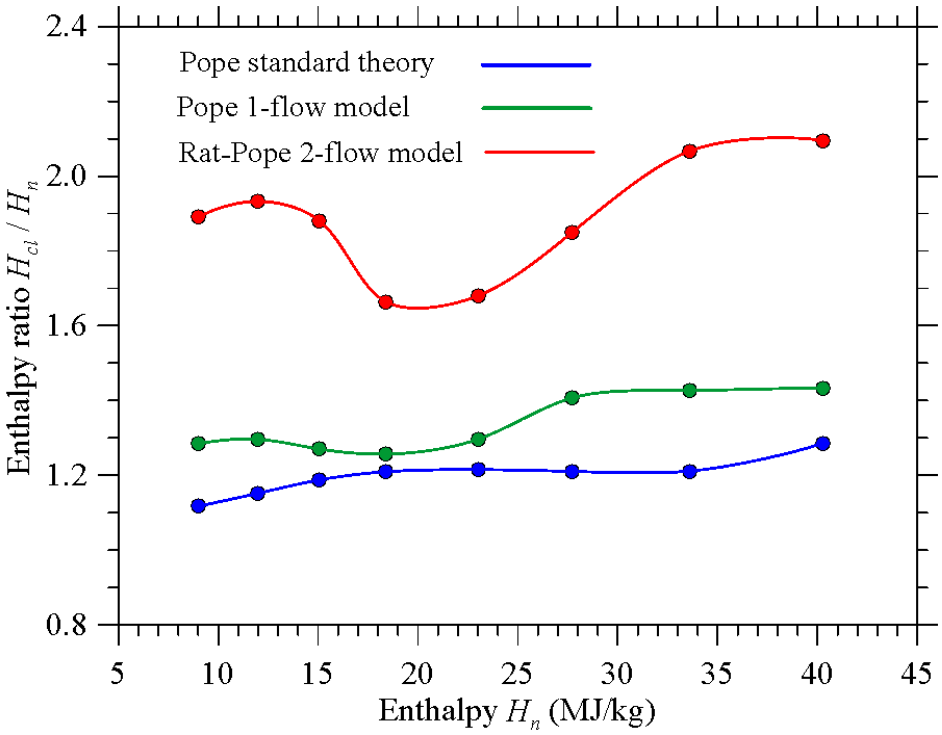

Figure 8: Enthalpy ratio as a function of H_n (the splines are used to guide the eye).

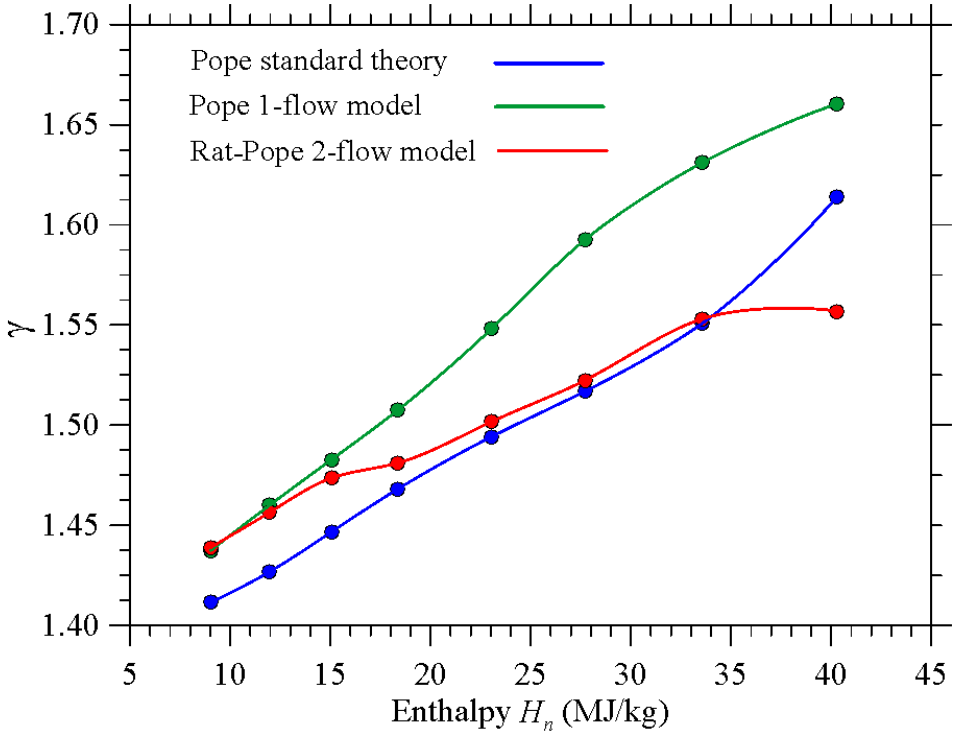

Figure 9: γ as a function of H_n (the splines are used to guide the eye).

Additionally, Fig. 10 shows a comparison between the isentropic coefficient γ calculated as:

1) $\gamma = C_p/C_v$, with C_p and C_v weighted averages of the respective values in the core and cold layer, in the Figure referred to as "Gamma-Rat";
2) By the well-known formulas by Vincenti and Kruger [5] for a chemically frozen mixture of atomic, diatomic and polyatomic species, with frozen vibrational energy, $\gamma = \frac{4+3Z}{4+Z}$ with $Z = 1 + \alpha$ and α total mass fraction of dissociated species.

The difference between the two coefficients is significant, with values from the Rat-Coudert model tending to remain closer to unity. This trend can be partly explained by the relatively low values predicted by CEA, which are even lower than those reported by Burm [10] for thermal plasmas, where ionization levels may exceed 10%.

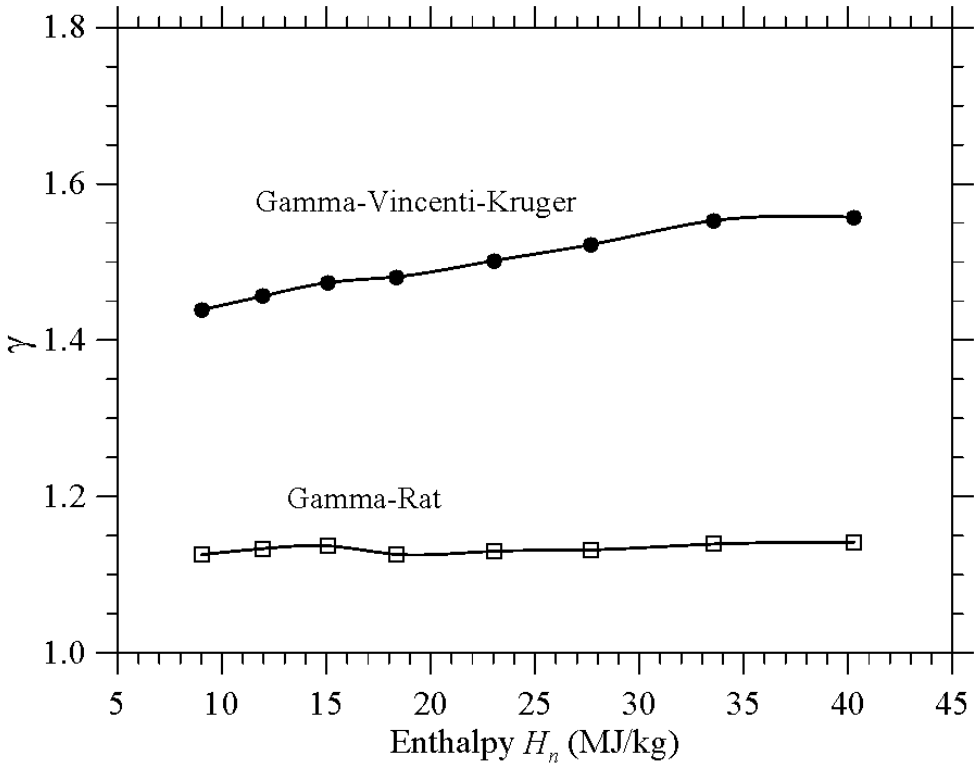

Figure 10: γ as a function of H_n (the splines are used to guide the eye).

4.1.3 *Supersonic Nozzle*

Figures 11 and 12 present a comparative assessment of Mach and Reynolds numbers obtained using the Pope and Rat-Coudert models, respectively. Overall, the agreement between the two formulations is relatively good for the Mach number, indicating a consistent prediction of the compressible expansion behavior across the two approaches. In contrast, a somewhat larger

discrepancy is observed for the Reynolds number, reflecting the higher sensitivity of this parameter to local variations in density and velocity fields.

The apparently anomalous Reynolds number observed at an enthalpy level of 40 MJ/kg can be rationalized by considering the coupled evolution of flow properties at the nozzle exit. In particular, this condition is characterized by a simultaneous increase in density and reduction in velocity, both of which directly influence the Reynolds number in opposite ways. The resulting balance between these competing effects leads to the observed non-monotonic behavior.

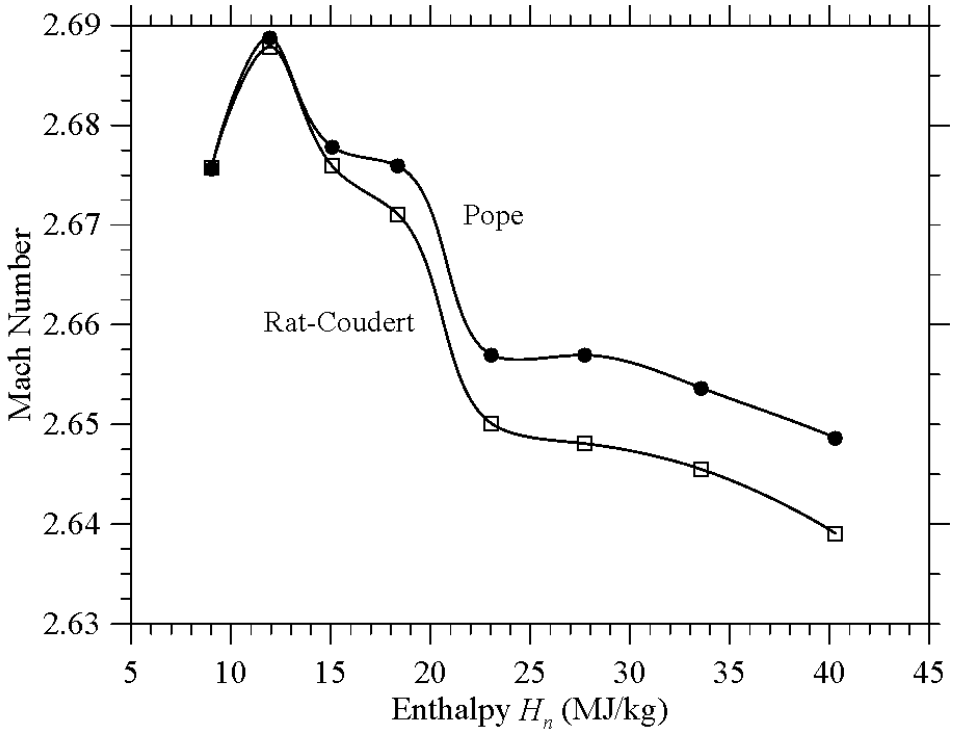

Figure 11: Mach number as a function of H_n (the splines are used to guide the eye).

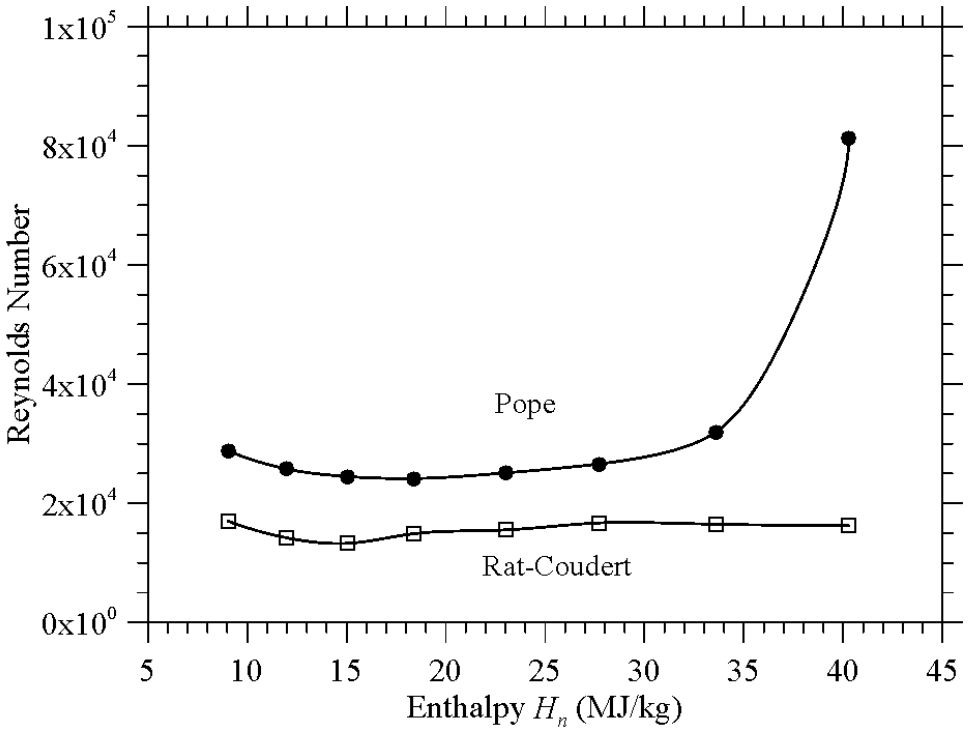

Figure 12: Reynolds number as a function of H_n (the splines are used to guide the eye).

5. CONCLUSIONS

The present study has introduced an extended framework for the characterization of high-enthalpy flows in arc-jet facilities operating under low-pressure reservoir conditions, with particular emphasis on reproducing atmospheric and planetary entry environments. Building upon the classical Frozen Sonic Flow Model (FSFM) originally formulated by Pope, a two-flow extension based on the Rat-Coudert representation of the plasma torch has been developed, enabling the explicit description of the intrinsic non-uniformity of arc-generated flows through a core-cold layer decomposition. This enhancement, combined with the application of the Pope model in the mixing chamber and standard isentropic relations in the nozzle, provides a unified and physically consistent description of the entire facility, from the arc heater to the supersonic exit section.

The numerical results obtained for nitrogen flows at a representative mass flow rate of 0.5 g/s and total enthalpy levels ranging between 10 and 40 MJ/kg have clearly demonstrated the impact of the proposed modeling hierarchy. In particular, we have shown systematic differences between the classical single-flow Pope formulation, the intermediate CEA-enhanced one-flow model, and the newly developed Rat-Pope two-flow approach. The classical formulation is shown to significantly underestimate the centerline enthalpy, while both improved formulations yield higher and more differentiated predictions, with the two-flow model capturing the strongest departure from the homogeneous assumption. These findings confirm that accounting

for ionization and radial flow non-uniformities at the torch exit plays a decisive role in the accurate reconstruction of downstream thermodynamic states.

Although some calculated values appears consistent with previous experimental evidence reported by Esposito and Lappa [4], where a single measured value of H_{cl}/H_n=1.33 was found using a supersonic total enthalpy probe and interpreted within the framework of Pope's theory, however, given the limited availability of experimental data, such agreement must be regarded as preliminary rather than conclusive.

A second important outcome concerns the discrepancy observed in the evaluation of the effective thermodynamic parameter γ, when comparing values obtained through the Vincenti–Kruger formulation with those derived from detailed CEA equilibrium calculations. This difference suggests that simplified thermodynamic closures may not fully capture the dynamics under the present operating conditions. This aspect is particularly relevant because γ directly influences both compressibility effects and nozzle expansion behavior, and therefore impacts the prediction of Mach number and Reynolds number in the test section. The possibility of experimentally determining γ and Mach number through combined measurements of total and static pressure using a dedicated total enthalpy probe provides another pathway for future work. In particular, targeted measurements of centerline enthalpy, pressure distributions, and derived thermodynamic quantities are essential to validate the predicted enhancement introduced by the two-flow formulation and to quantify its accuracy across different operating regimes.

6. REFERENCES

[1] Winovich W., (1964), On the equilibrium sonic-flow method for evaluating electric-arc air-heater performance, NASA TN D-2132.

[2] Jorgensen L. H., The total enthalpy of a one-dimensional nozzle flow with various gases, NASA TN D-2233 (1964)

[3] Pope R. B., (1968), Measurements of enthalpy in low-density arc-heated flows, AIAA J., 6(1), 103-110.

[4] Esposito A. and Lappa M., (2020), "Experimental and Theoretical Verification of the Frozen Sonic Flow Method for Mixtures of Polyatomic Gases", AIAA Journal, vol 58 n. 1, pp. 265–277

[5] Vincenti W.G. and Kruger C.H., (1965), Introduction to Physical Gas Dynamics, John Wiley & Sons, New York, 1965.

[6] Rat V. and Coudert J. F., (2006), "A simplified analytical model for dc plasma spray torch: influence of gas properties and experimental conditions" J. Phys. D: Appl. Phys. 39, 4799–4807 doi:10.1088/0022-3727/39/22/010

[7] Brown S. C. "Basic Data of Plasma Physics", John Wiley and Sons, 1959, pp.318 -321

[8] Sanford G. and McBride B.J., (1994), "Computer Program for Calculation of Complex Chemical Equilibrium Compositions and Applications I. Analysis", NASA RP-1311, 1994.

[9] Stull, D. R. (1965). JANAF Thermochemical Tables.. (Vol. 1). Clearinghouse.

[10] Burm, K. T. A. L., Goedheer, W. J., and Schram, D. C. (1999). The isentropic exponent in plasmas. Physics of Plasmas, 6(6), 2622-2627.

[11] Gordon S. and Mcbride B.J. (1994), “Computer program for calculation of complex chemical equilibrium compositions and applications. Part 1: Analysis » NASA-RP_1311,October 1, 1994